

Discretization of Icosahedral Grids on the Sphere

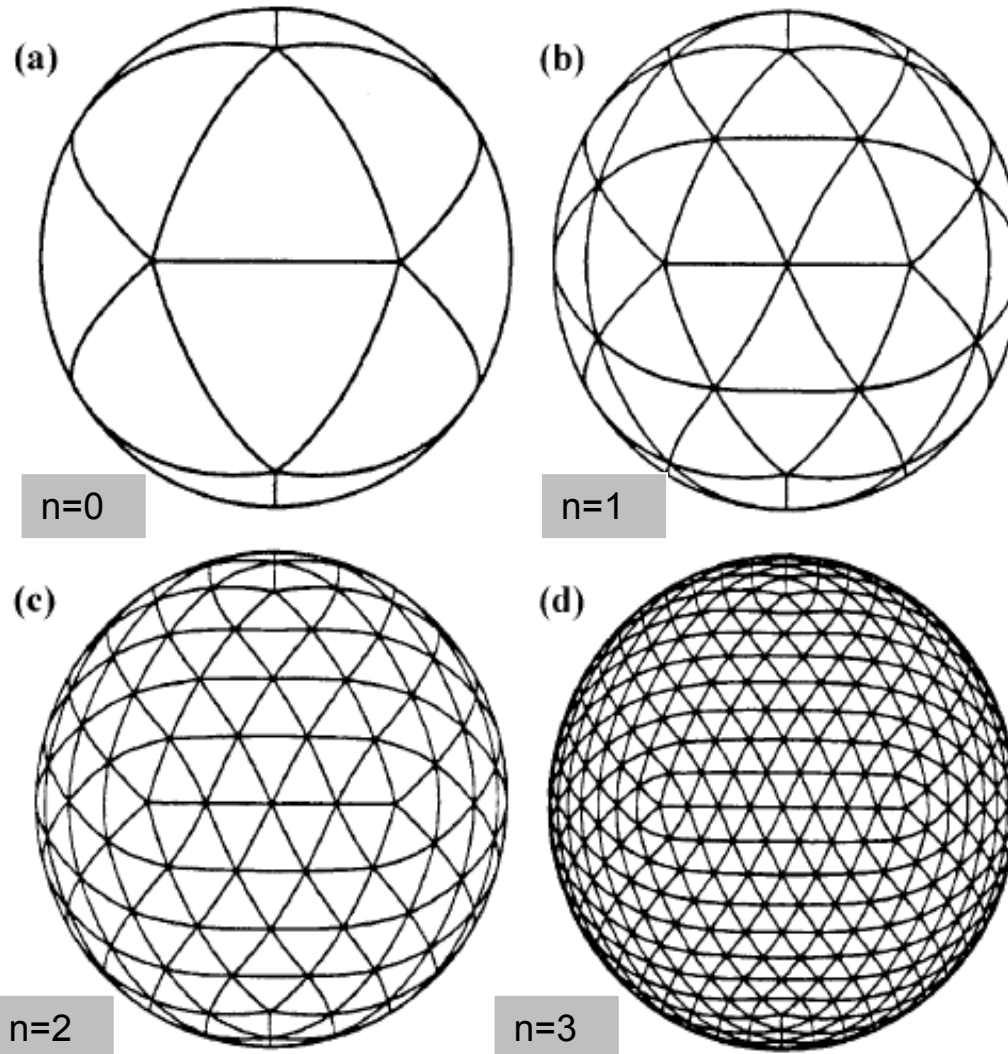
Jin Lee @ GSD/ESRL



Outline of this talk

- Local .vs. Spherical coordinates
- Icosahedral-hexagonal grid inhomogeneity, grid noises, and optimizations: Impacts on numerical accuracy.
- Icosahedral grid descretization and TEs.
- Results on the use of f.-v. Icosahedral model for weather forecasts; FIM and NIM (non-hydrostatic Icosahedral model).
- Preliminary results on NIM
- Numerical ssues related to Icosahedral grid descretizations.

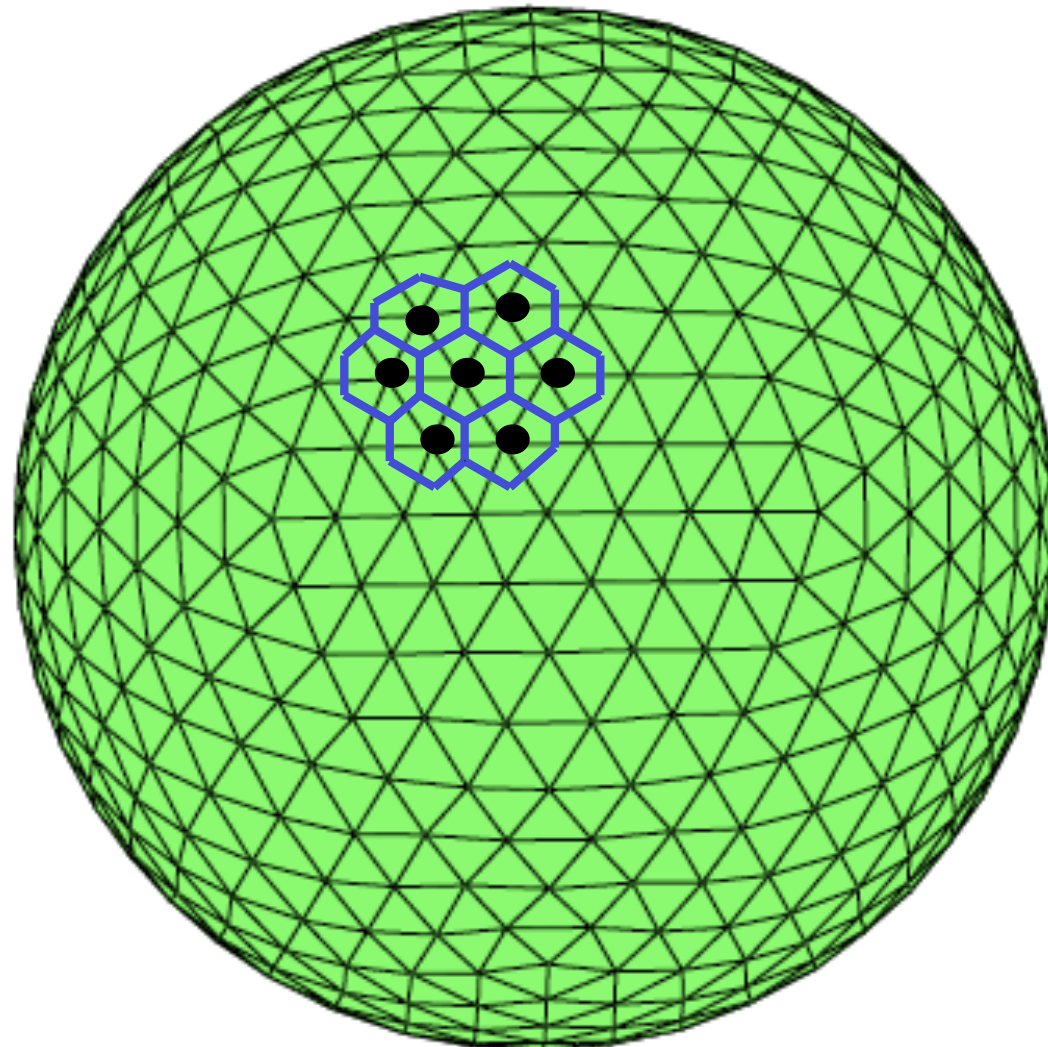
What Is An Icosahedral Model



$N=((2^{**n})^{**2})^*10 + 2$; 5th level – $n=5 \rightarrow N=10242 \sim 240\text{km}$; $\max(d)/\min(d) \sim 1.2$
6th level – $n=6 \rightarrow N=40962 \sim 120\text{km}$; 7th level – $n=7 \rightarrow N=163842 \sim 60\text{km}$
8th level – $n=8 \rightarrow N=655,362 \sim 30\text{km}$; 9th level – $n=9 \rightarrow N=2,621,442 \sim 15\text{km}$
10th level ~7.km; 11th level ~3.5km , 12th level ~1.7km

Icosahedral-Hexagonal Grid

(Voronoi corner points)



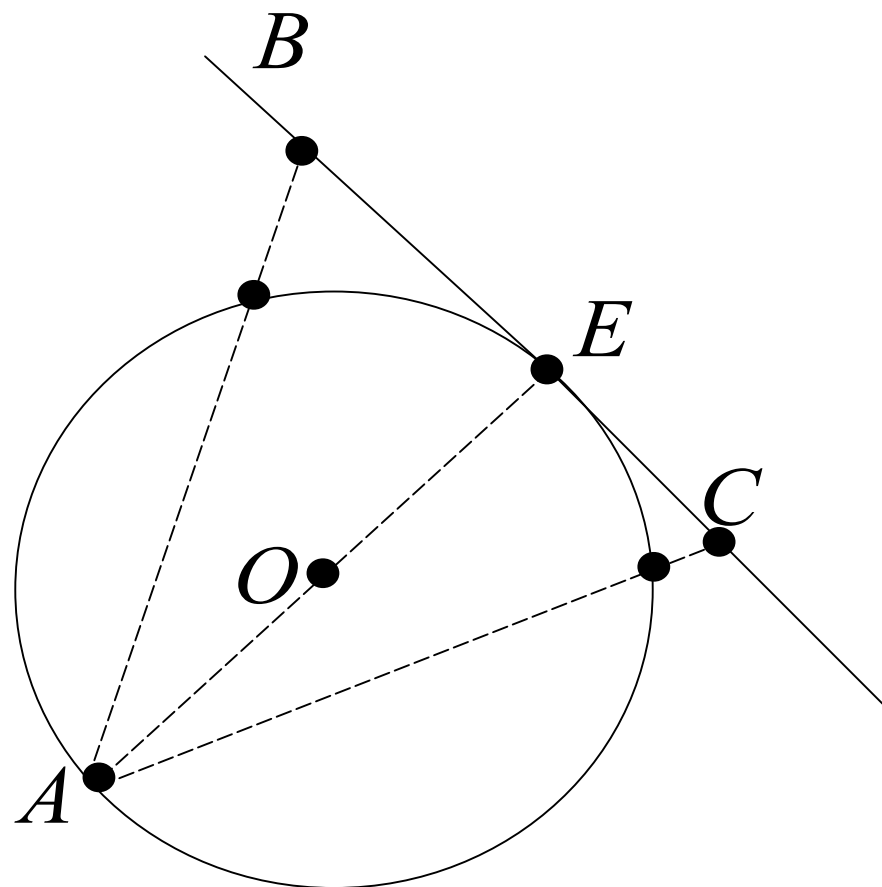
Choice of coordinates for geodesic grids

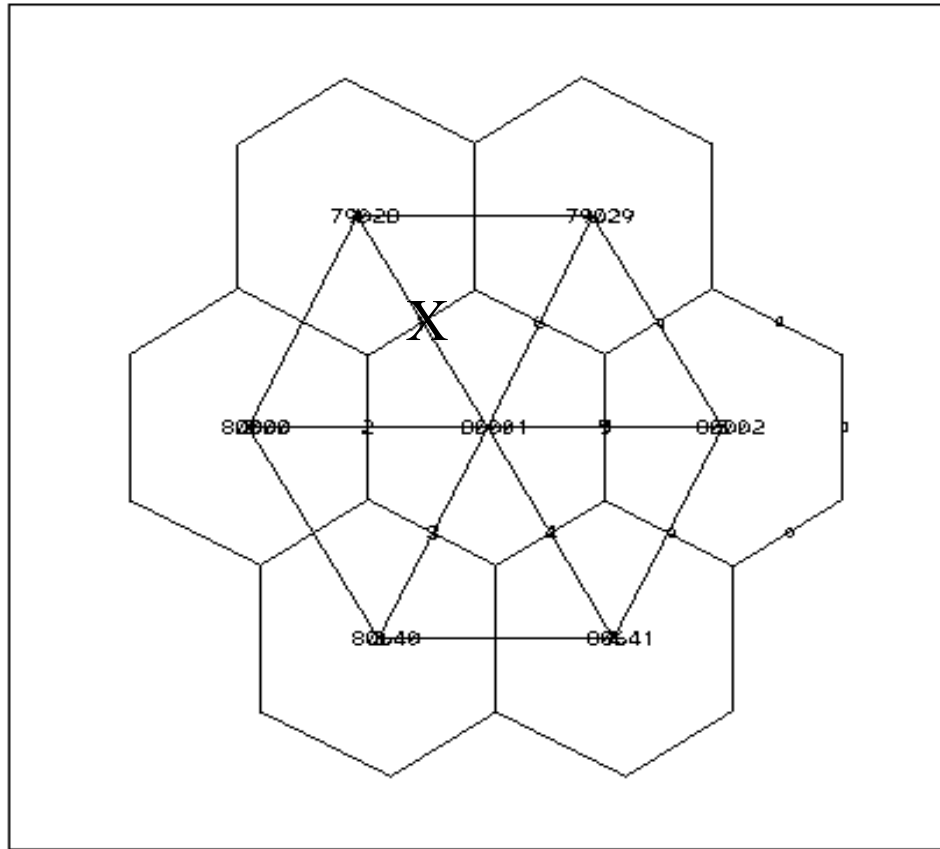
Spherical .vs. Local coord.

(ping pong .vs. golf balls)



General Stereographic Projection





Finite volume flux computation:

- flux in/out each cell from surrounding donor cells

Polynomial interpolation of $(n + 1)$ points means that

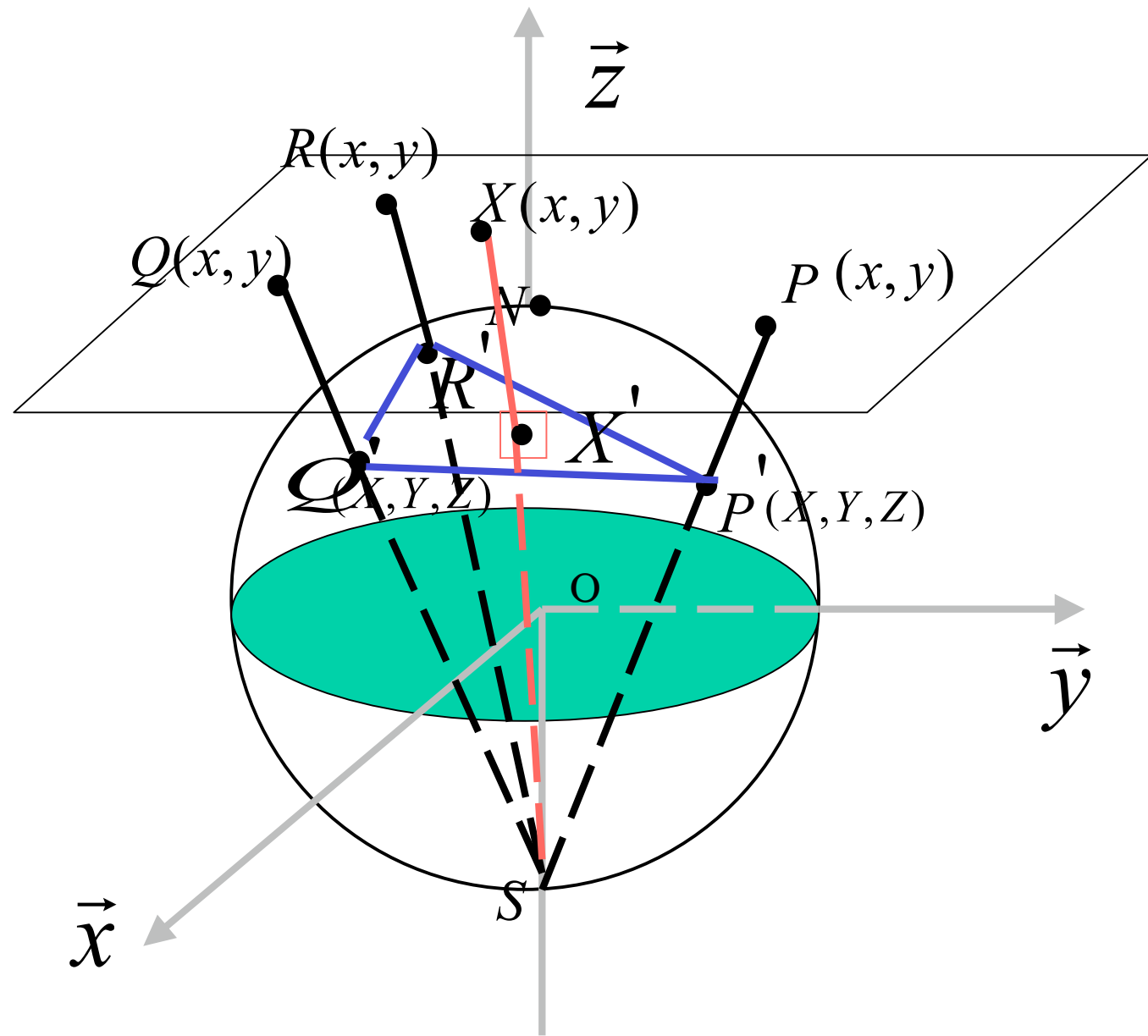
$$f(x) = a_0 + a_1x + a_2x^2 + \dots + a_{n-1}x^{n-1} + a_nx^n$$

It can be written in a matrix - vector form as follow :

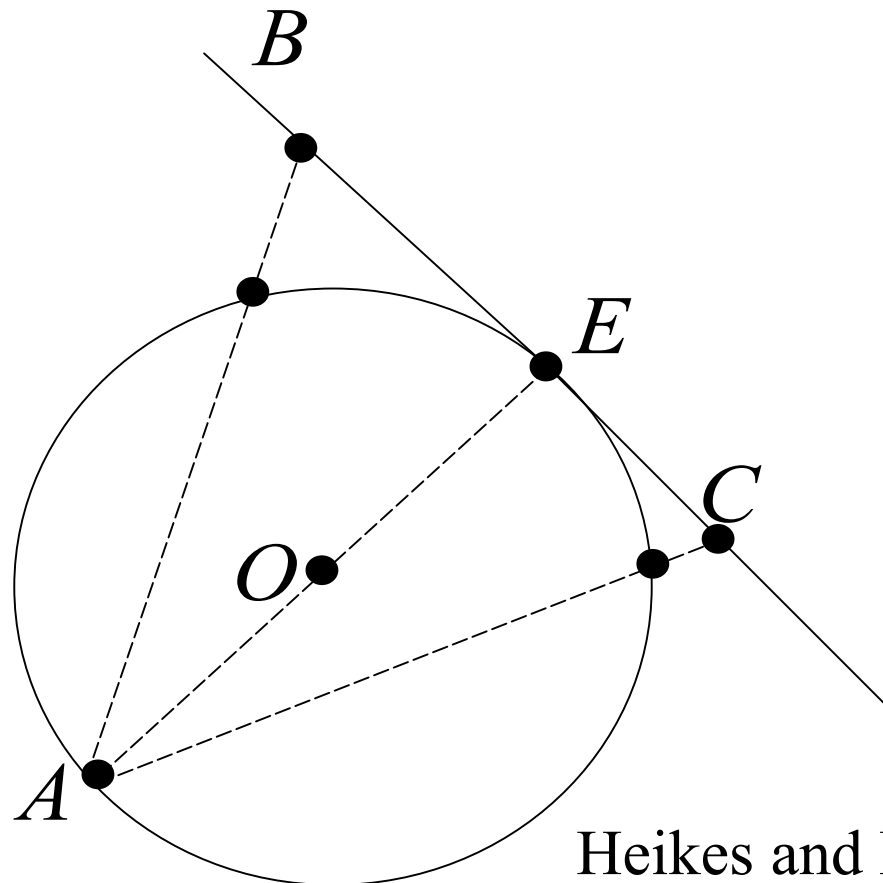
$$\left[\begin{array}{cccccc|c} 1 & x_1 & x_1^2 & \cdots & \cdots & x_1^{n-1} & x_1^n & a_0 \\ 1 & x_2 & x_2^2 & \cdots & \cdots & x_2^{n-1} & x_2^n & a_1 \\ 1 & x_3 & x_3^2 & \cdots & \cdots & x_3^{n-1} & x_3^n & a_2 \\ \vdots & \vdots & \vdots & \cdots & \cdots & \vdots & \vdots & \vdots \\ \vdots & \vdots & \vdots & \cdots & \cdots & \vdots & \vdots & \vdots \\ 1 & x_{n-1} & x_{n-1}^2 & \cdots & \cdots & x_{n-1}^{n-1} & x_{n-1}^n & a_{n-1} \\ 1 & x_n & x_n^2 & \cdots & \cdots & x_n^{n-1} & x_n^n & a_n \end{array} \right] = \left[\begin{array}{c} f_0 \\ f_1 \\ f_2 \\ \vdots \\ \vdots \\ f_{n-1} \\ f_n \end{array} \right]$$

$\brace{ \text{Vandermonde Matrix}}$

A simple 2 - D example : $f(x, y) = a_1 + a_2x + a_3y$



General Stereographic Projection



Heikes and Randall(1995): used 6-pts stencils on sphere for VDMN with a recursive procedure to establish coplanar stencil points.

Justification (ii),

The 2-D operator applied to the straight lines, rather than the 3-D operator along the curved lines, e.g.,

Stoke's theorem:

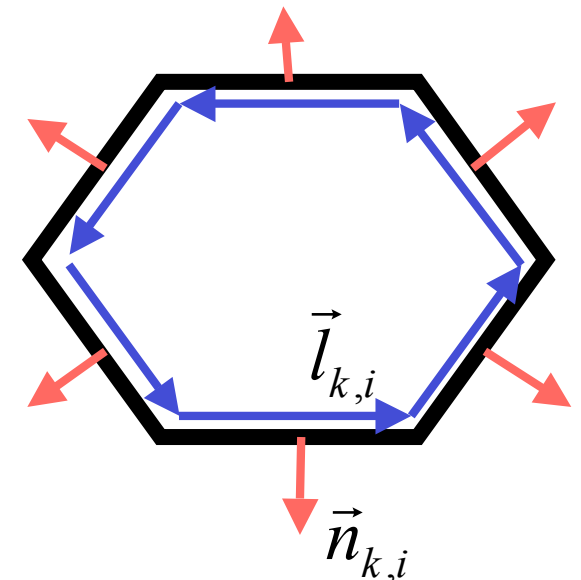
$$\zeta = \int_A (\nabla_h \times \vec{V}_h) dA = \oint_s (\vec{V}_h \cdot \vec{l}) ds$$

$$\zeta_k = \frac{1}{A_k} \sum_{i=1}^n \left(\frac{\vec{V}_{k,i} \cdot \vec{l}_{k,i}}{\mathbf{m}_{k,i}} \right) \Delta S_{k,i}$$

Divergence theorem :

$$\int_A (\nabla_h \cdot \vec{V}_h \phi) dA = \oint_s (\vec{V}_h \phi \cdot \vec{n}) ds$$

$$\delta_{\phi(k)} = \frac{1}{A_k} \sum_{i=1}^n \left(\frac{\phi_{k,i} \vec{V}_{k,i} \cdot \vec{n}_{k,i}}{\mathbf{m}_{k,i}} \right) \Delta S_{k,i}$$



Justification (iii): Reduce the number of basis functions in Vandermonde matrix.

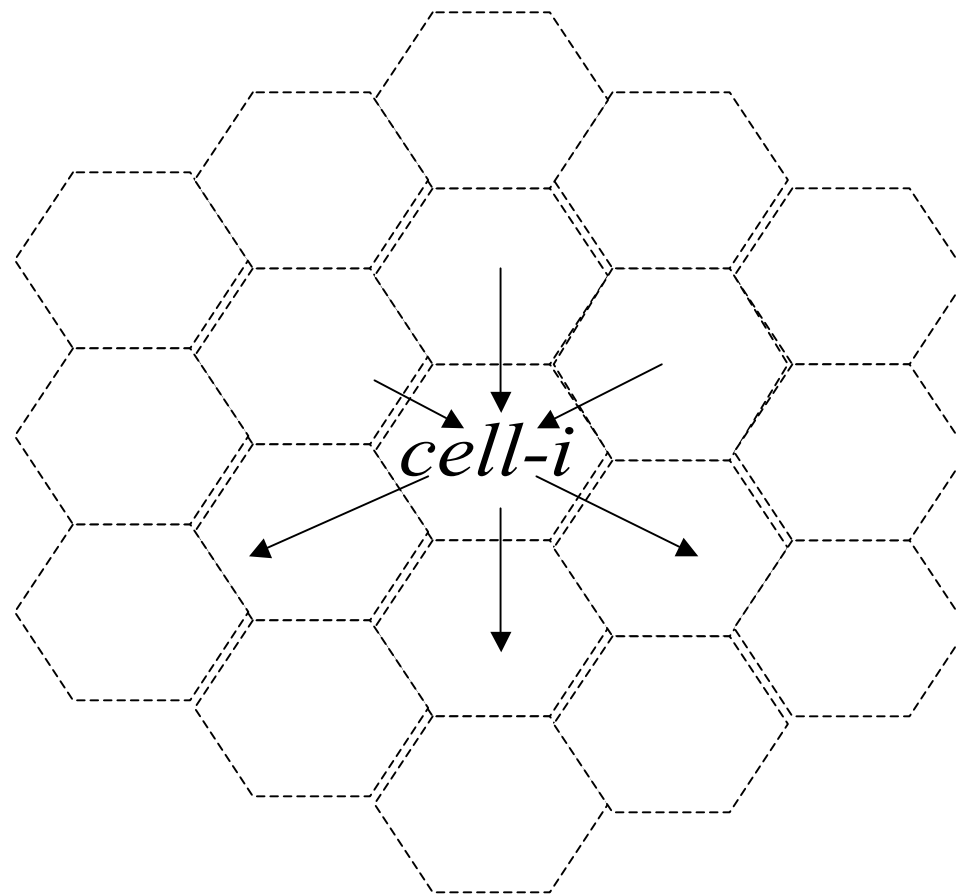
$$\underbrace{\begin{bmatrix} 1 & x_1 & x_1^2 & \cdots & \cdots & x_1^{n-1} & x_1^n \\ 1 & x_2 & x_2^2 & \cdots & \cdots & x_2^{n-1} & x_2^n \\ 1 & x_3 & x_3^2 & \cdots & \cdots & x_3^{n-1} & x_3^n \\ \vdots & \vdots & \vdots & \cdots & \cdots & \vdots & \vdots \\ \vdots & \vdots & \vdots & \cdots & \cdots & \vdots & \vdots \\ 1 & x_{n-1} & x_{n-1}^2 & \cdots & \cdots & x_{n-1}^{n-1} & x_{n-1}^n \\ 1 & x_n & x_n^2 & \cdots & \cdots & x_n^{n-1} & x_n^n \end{bmatrix}}_{\text{Vandermonde Matrix}} = \begin{bmatrix} a_0 \\ a_1 \\ a_2 \\ \vdots \\ a_{n-1} \\ a_n \end{bmatrix} = \begin{bmatrix} f_0 \\ f_1 \\ f_2 \\ \vdots \\ f_{n-1} \\ f_n \end{bmatrix}$$

Justification (iv): It requires only a few extra fast product operators (~DWD MWR 2000: rotate with two great circles)

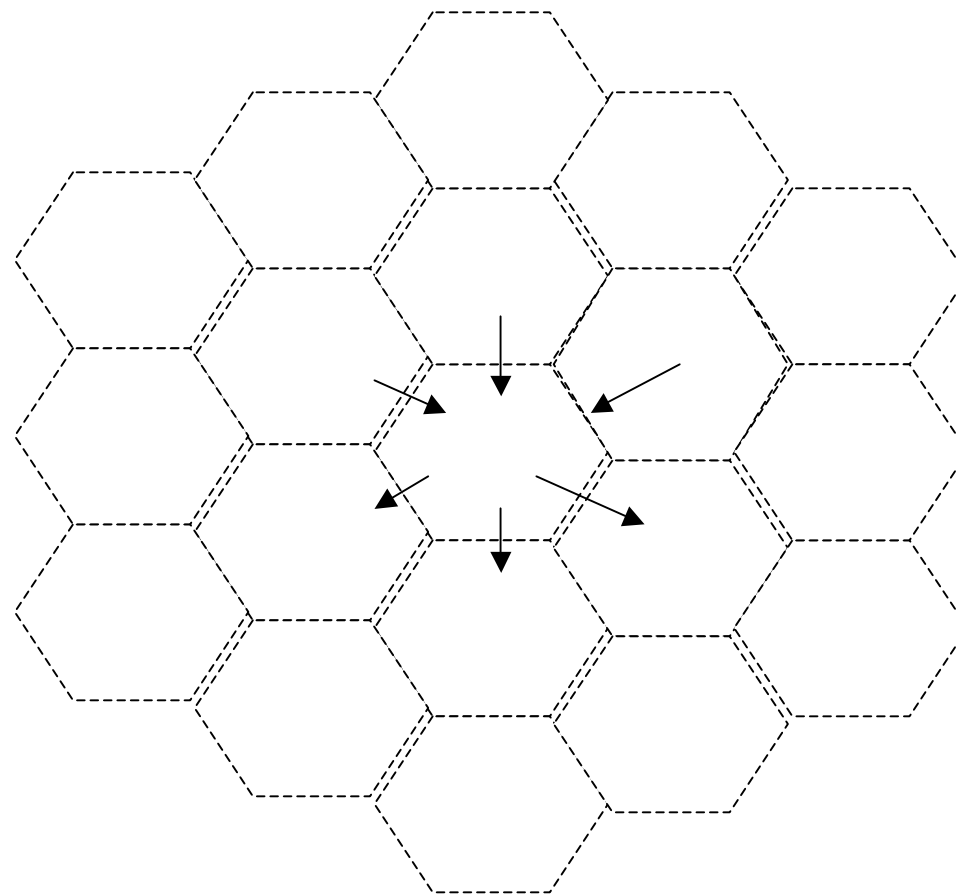
Monotonicity and Positive Definiteness on Icos-grids with AB 3rd scheme

Flux-Correct-Transport (Zalesak, 1979)

Compute high order fluxes
 flx_h over all edges
in the domain.



Compute low order fluxes
 f_{lxl} over all edges
in the domain.

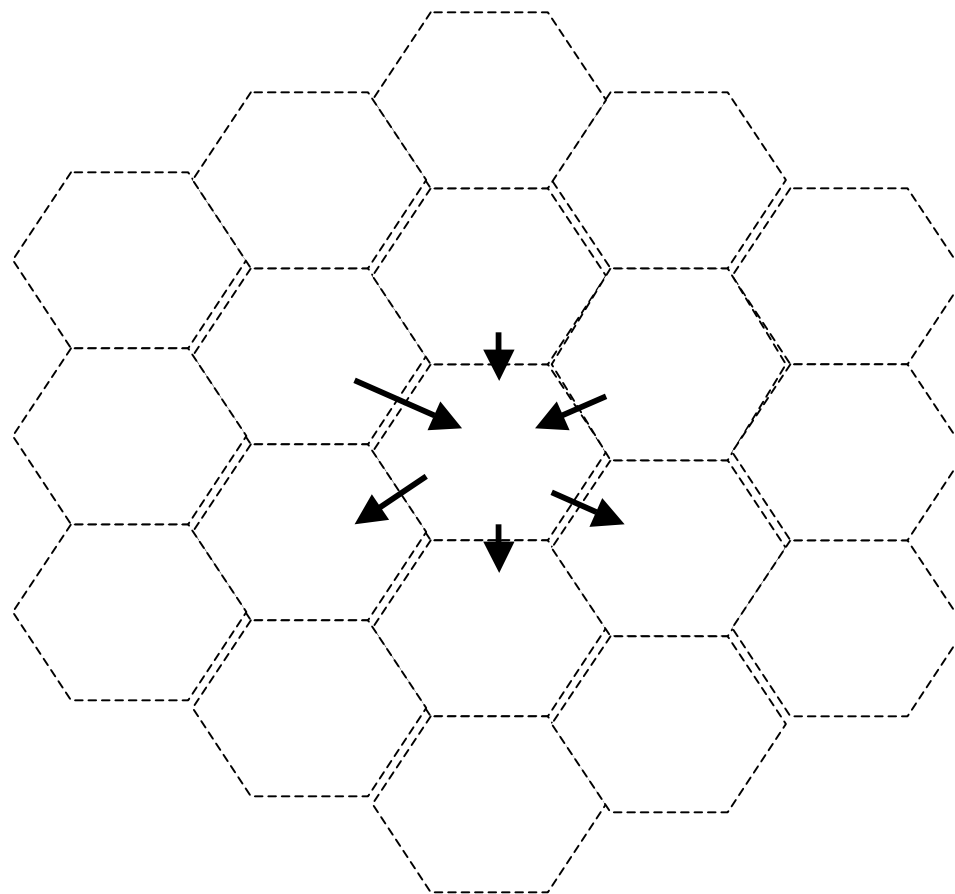


Define antidiffusive fluxes

$$fad = flxh - flxl$$

over all edges

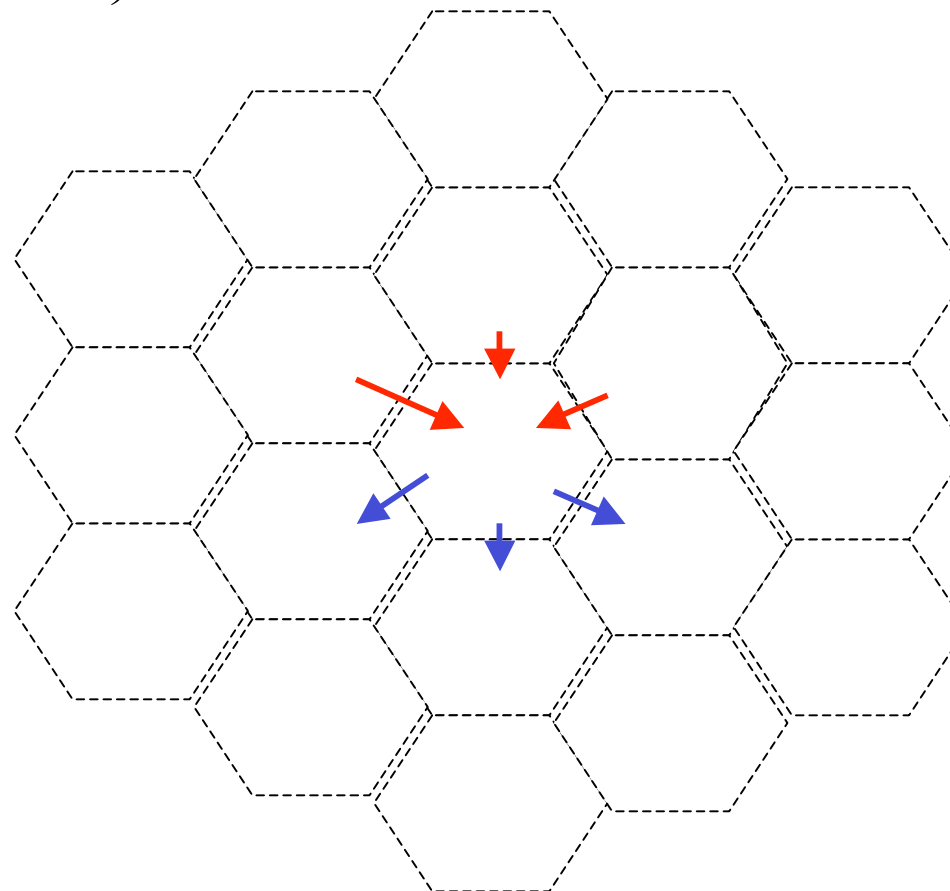
in the domain.



Group antidiffusive fluxes as

In – fluxes(in red) and

out – fluxes(in blue).

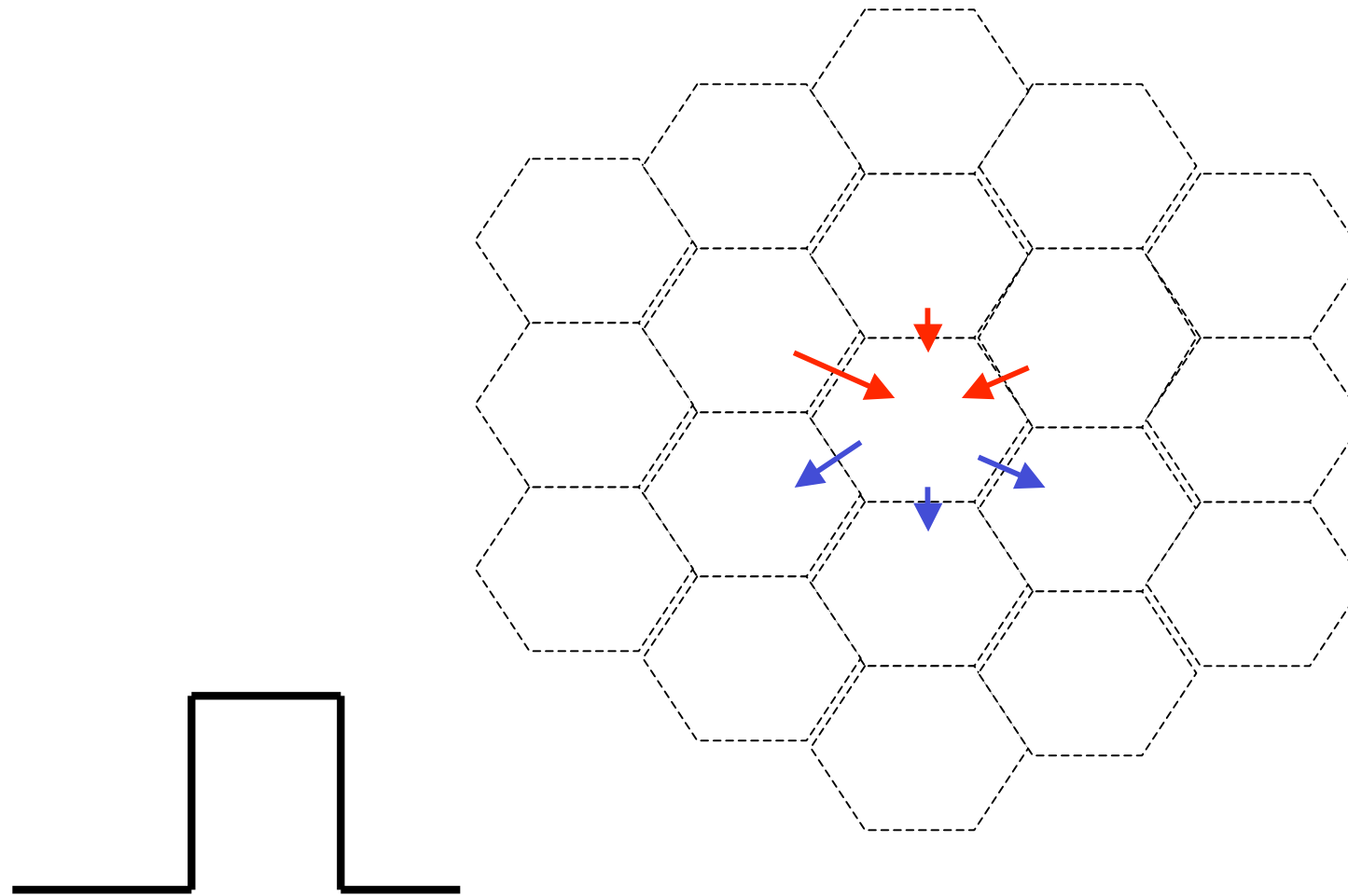


Group antidiffusive fluxes as

In – fluxes(in red) and

out – fluxes(in blue).

(2 - D formulation, no directional splitting)



Icosahedral SWE :

$$\begin{cases} \frac{\partial u}{\partial t} - (f + \zeta)v + m \frac{\partial(E_k + \phi)}{\partial x} = 0 \\ \frac{\partial v}{\partial t} + (f + \zeta)u + m \frac{\partial(E_k + \phi)}{\partial y} = 0 \\ \frac{\partial \phi}{\partial t} + m^2 \left[\frac{\partial}{\partial x} \left(\frac{\phi u}{m} \right) + \frac{\partial}{\partial y} \left(\frac{\phi v}{m} \right) \right] = 0 \end{cases}$$

where, ζ : vorticity, $E_k = \frac{u^2 + v^2}{2}$

Numerics of the Icosahedral SWM

- Each Icosahedral cell is solved on a local coordinate.
- Model variables are defined on a non-staggered A-grid.
- Vandermonde Interpolation to estimate edge variables.
- All differentials evaluated as line integrals around the cells using finite-volume conservative discretization.
- Grid points in a linear horizontal loop that allow any horizontal point sequence
- Explicit 3rd-order Adams-Bashforth time differencing.
- Flux Corrected Transport formulated based on the high-order (3rd Order) Adams-Bashforth scheme to maintain conservative positive definite transport.

Issues of Grid In-homogeneity

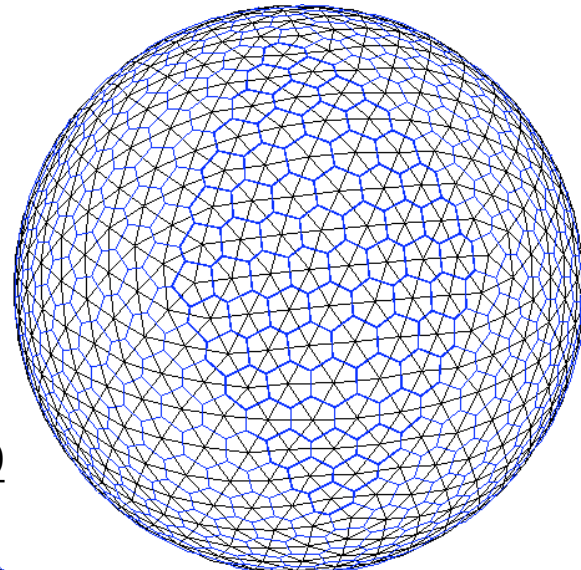
**Grid optimization/
impact on numerical accuracy**

Geometric properties of Icosahedral-Hexagonal grid on sphere (in preparation)

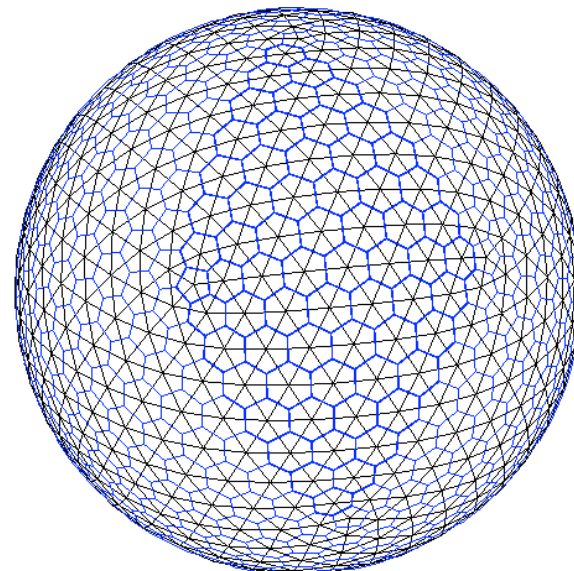
Ning Wang and Jin Lee

Comparisons of three Icosa-grids

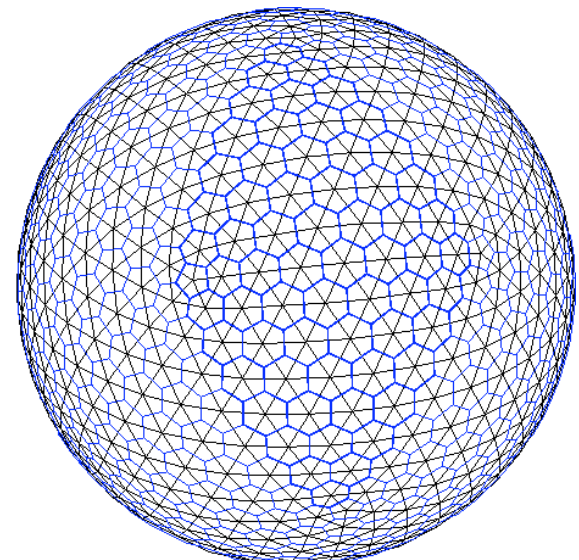
STD: Edge_max/min=1.84



SPN: Edge_max/min=1.30



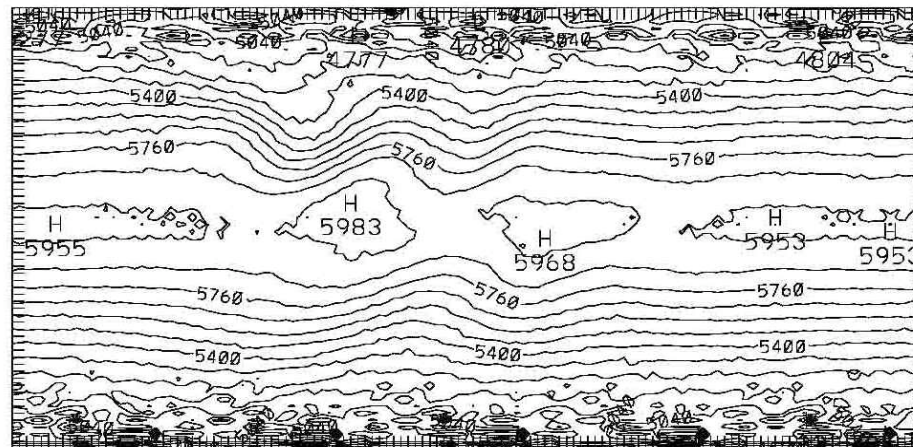
MGC: Edge_max/min=1.32



Williamson et al.(1992) Case V: Zonal flow over Mountain

PHI (6 DAY)

STD



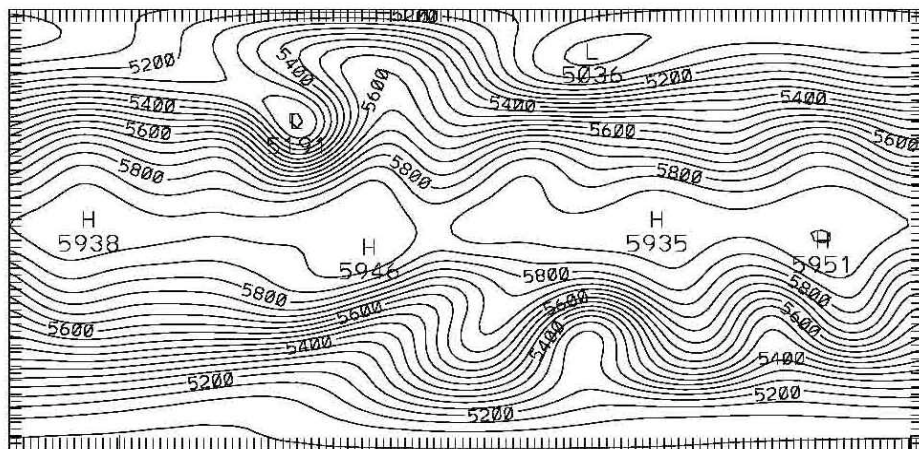
CONTOUR FROM 4410.0 TD 5948.0 CONTOUR INTERVAL OF 90.000 PT(3,3)= 4958.3

PHI (15 DAY)

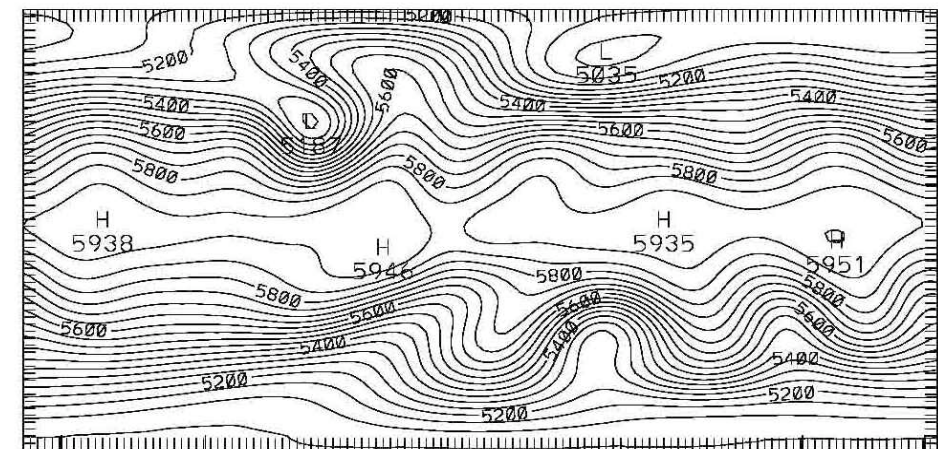
SPN

PHI (15 DAY)

MGC



CONTOUR FROM 5000.0 TD 5958.0 CONTOUR INTERVAL OF 50.000 PT(3,3)= 5051.1



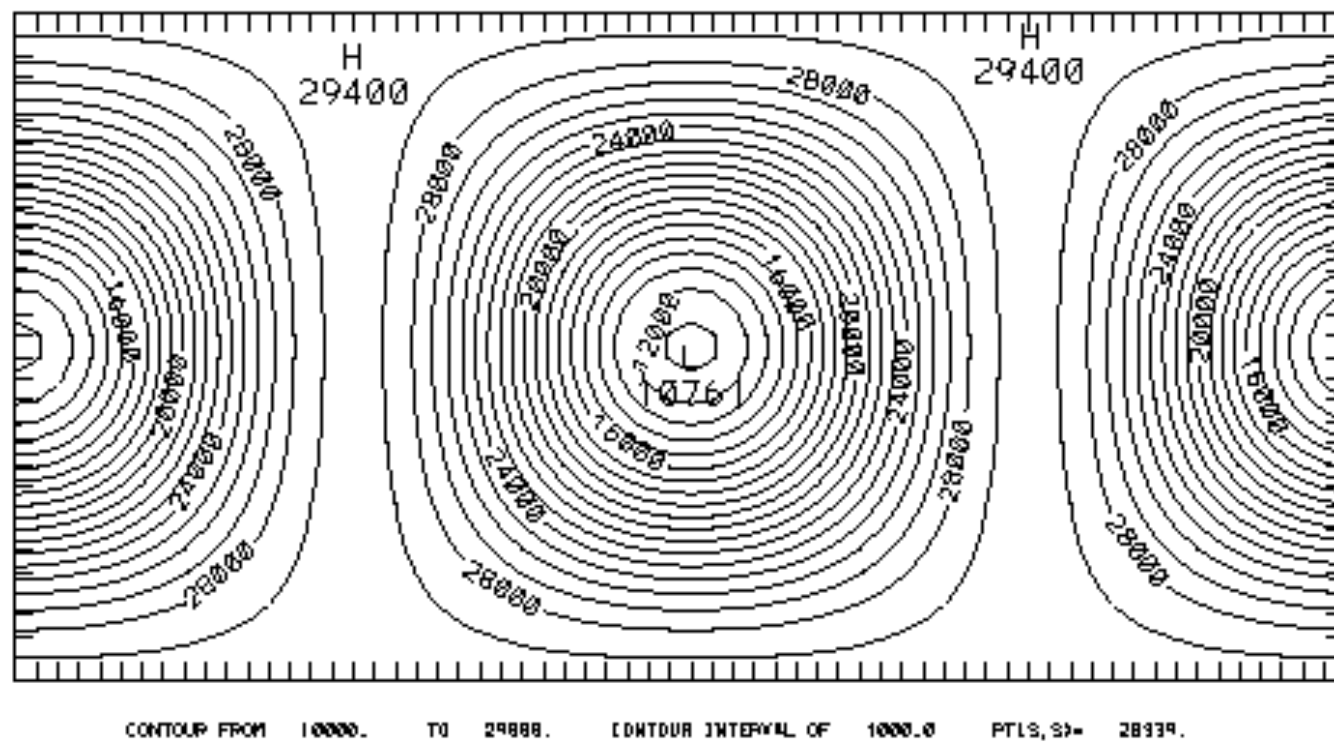
CONTOUR FROM 5000.0 TD 5958.0 CONTOUR INTERVAL OF 50.000 PT(3,3)= 5052.1

Grid Noises / TEs Convergence

**Grid optimization/
impact on numerical accuracy**

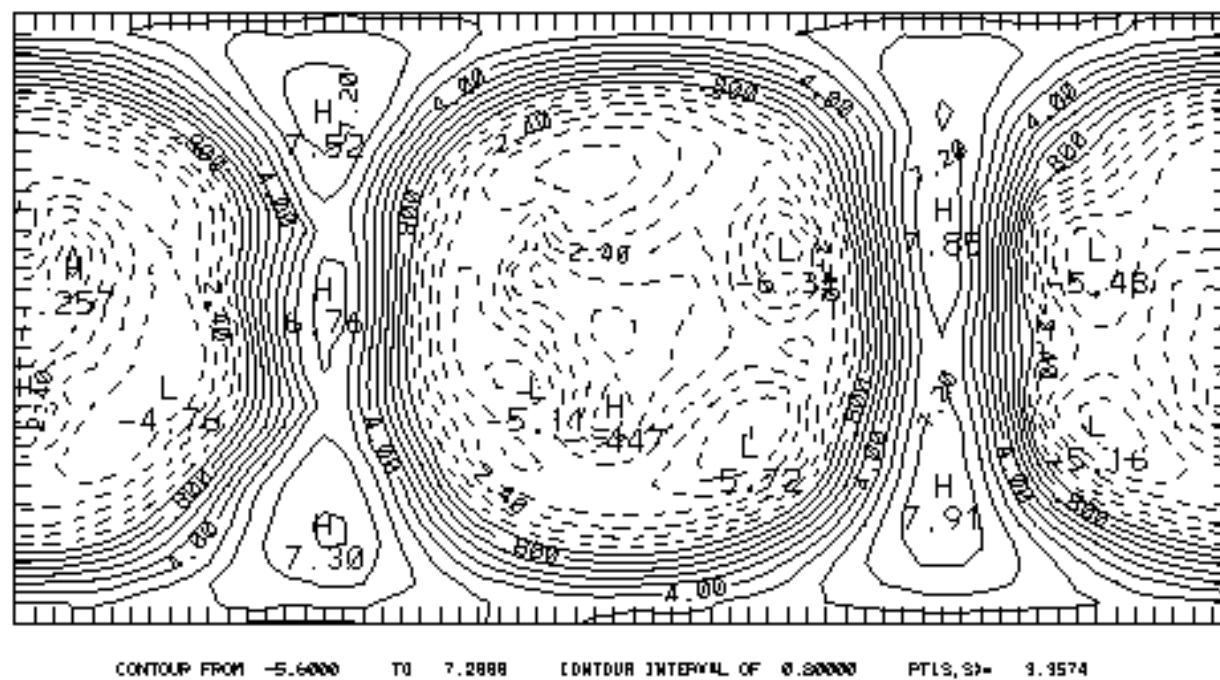
CASE II (steady state nonlinear geostrophic flow)

PHI (0 DAY I

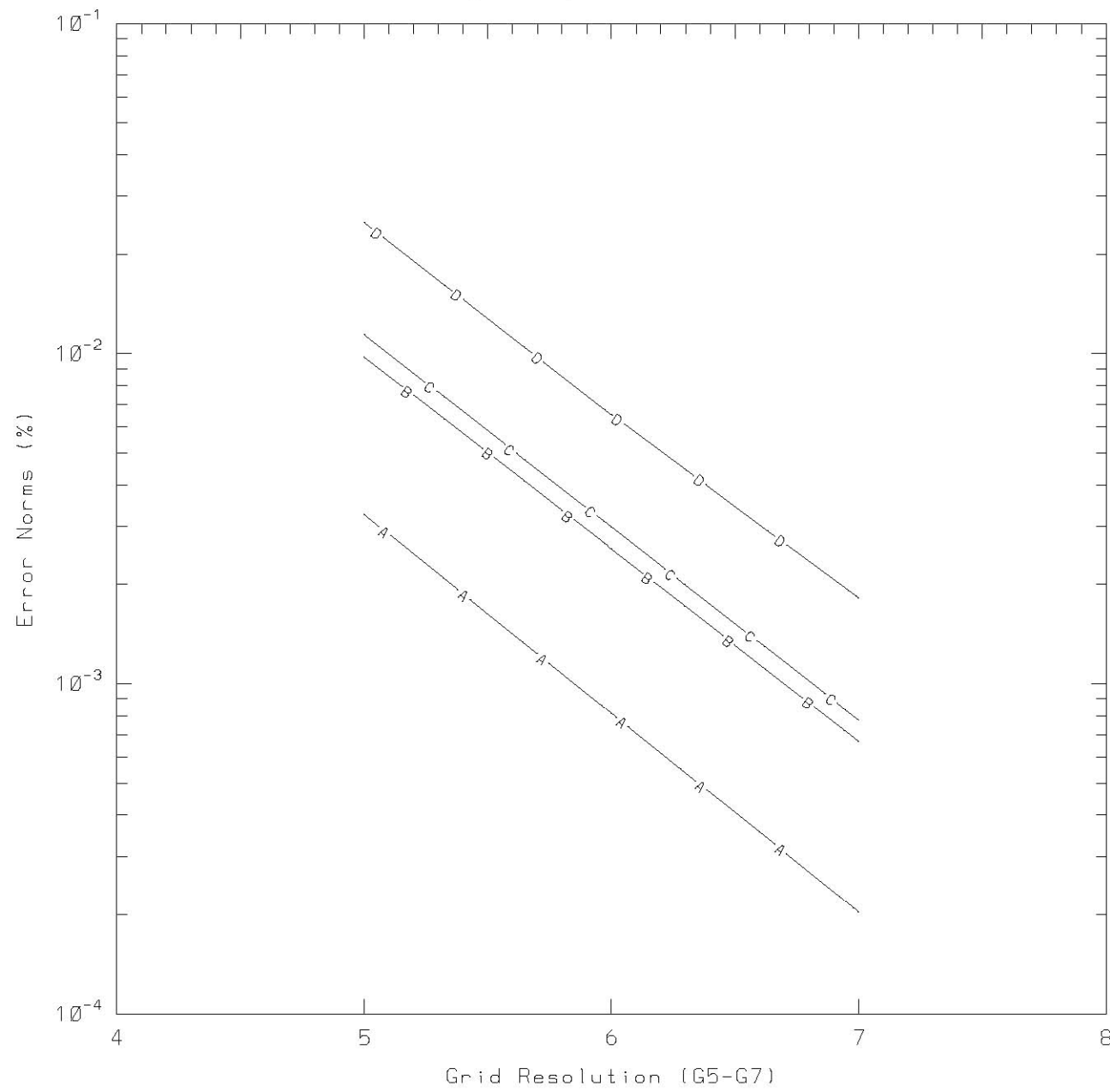


DP (1 DAY)

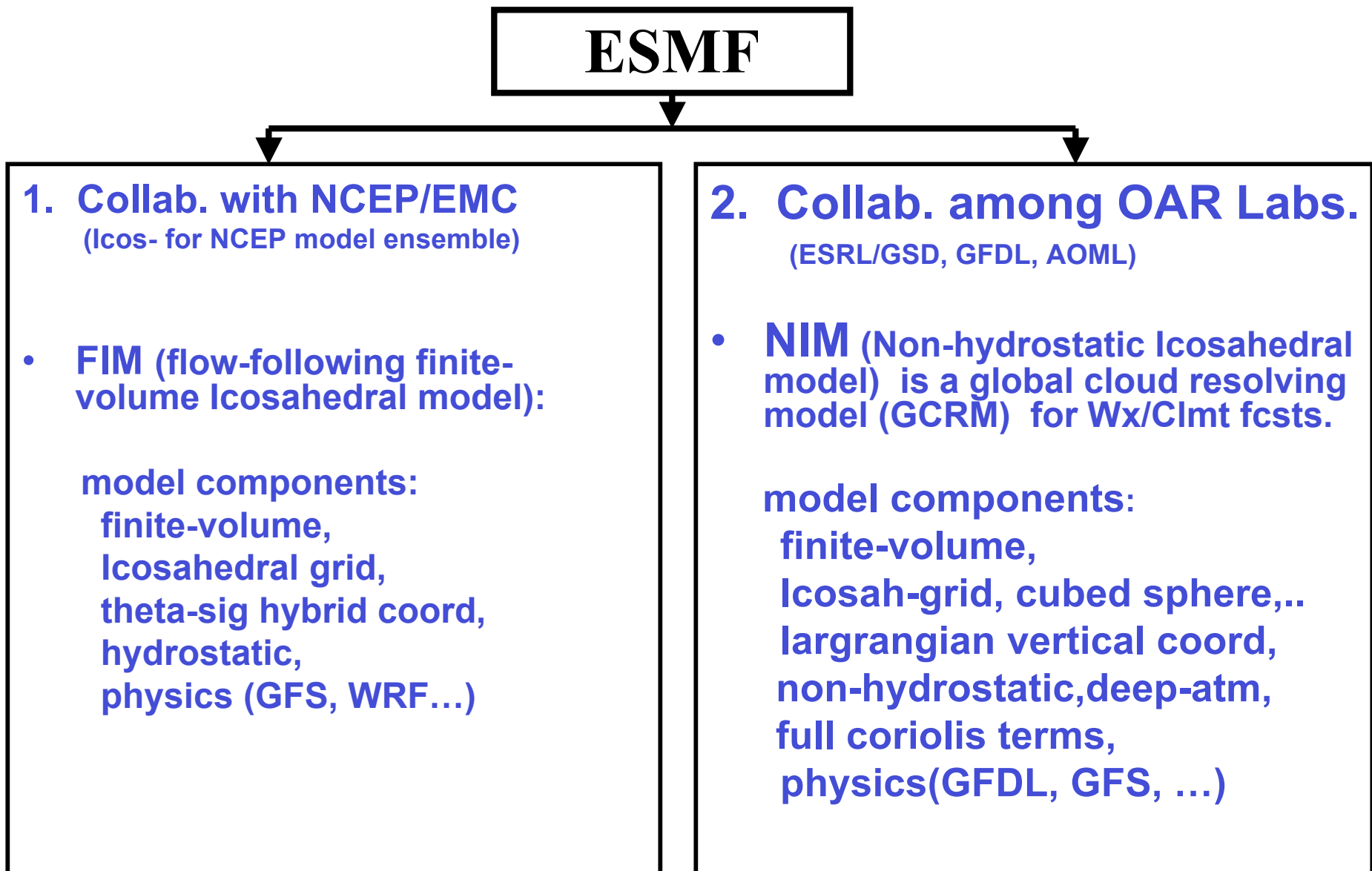
Vandermonde@G5



Phi : A: Analy slope B(L1)/C(L2)/D(Linf)



FIM and NIM model components



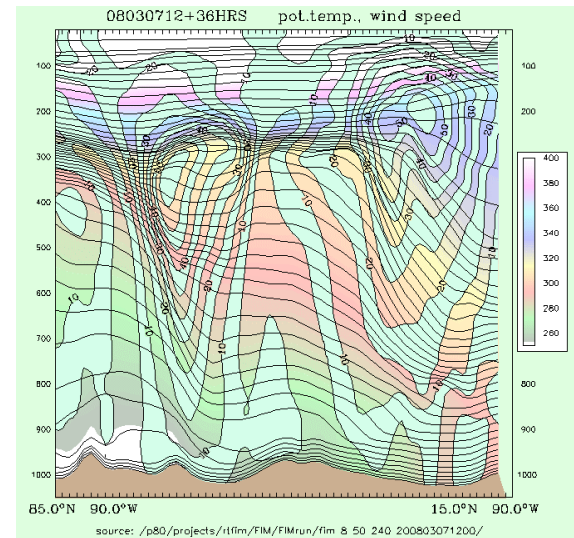
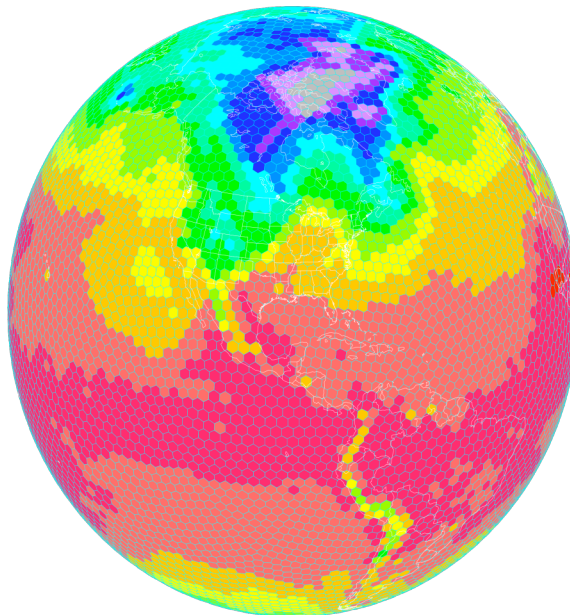
FIM model/ system

-Contributors

FIM DESIGN

Jin Lee
Sandy MacDonald
Rainer Bleck

Jian-Wen Bao
John M. Brown
Jacques Middlecoff
Ning Wang
Stan Benjamin



Tom Henderson	ESMF, Subversion
Chris Harrop	WorkFlow Manager, xml real-time scripts
Bill Moninger Brian Jamison Susan Sahm Ed Szoke	Verification, Web page, Evaluation
Georg Grell	FIM- chemistry, aerosols

FIM display
capabilities for
Mary Glackin visit

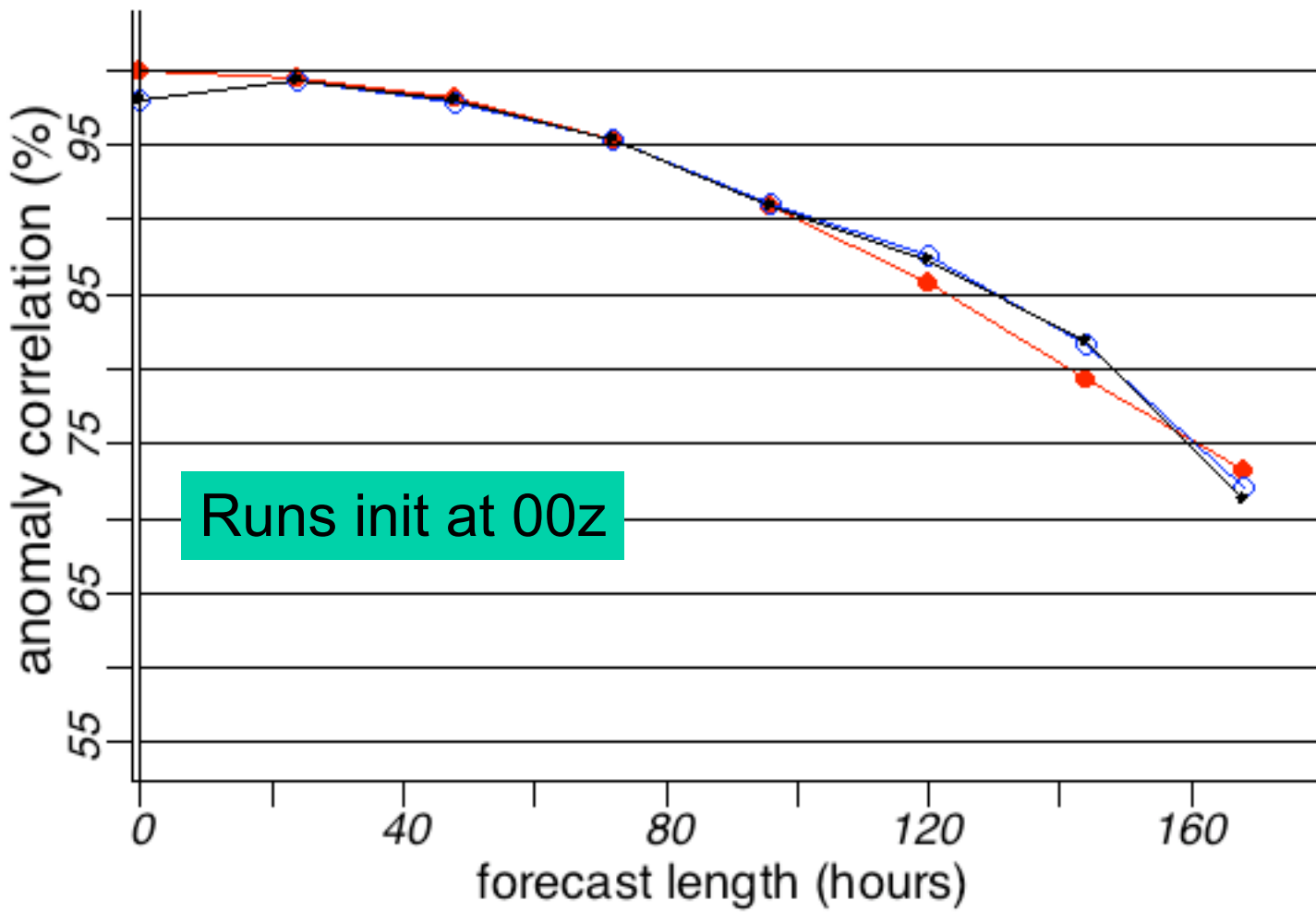
Bob Lipschutz
David Himes
Beth Russell
Steve Albers
Tom Kent
+ dozens more...

Results on the use of f.-v. Icosahedral model for weather forecasts

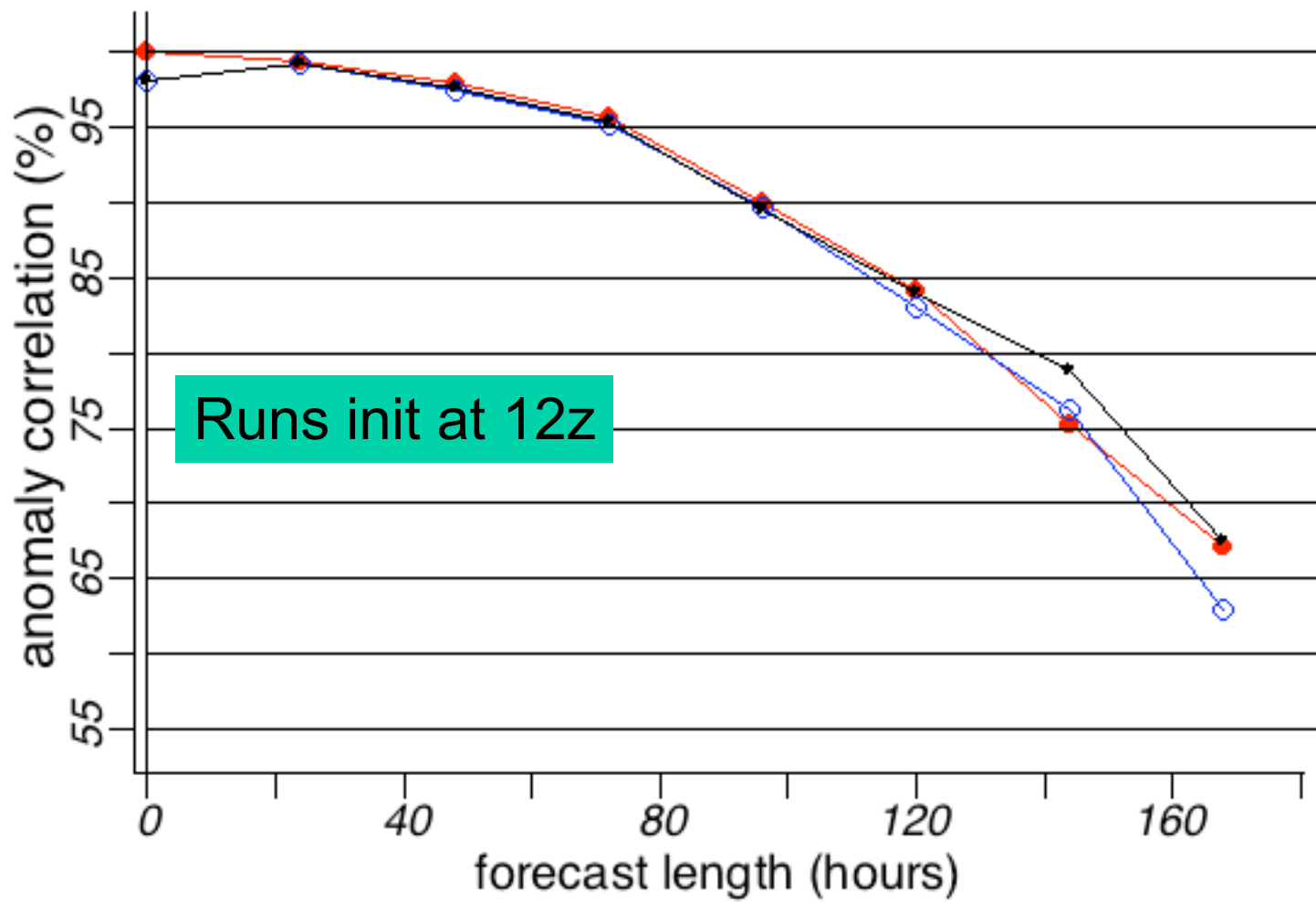
**FIM real time forecasts initialized with GFS initial
condition at 00 and 12 UTC**
(comparisons of FIM and GFS 500 mb ACC)

- Interpolate GFS initial data to Icosahedral grid.
- Perform hydrostatic initialization.
- Perform 7-day fcst with $dx \sim 30\text{km}$ without explicit dissipation.
- Experimental FIM runs with $dx \sim 15\text{km}$ resolution.
- Same initial condition, terrain & sfc parameters, physics package running at similar model resolutions ($dx \sim 30\text{ km}$)

- FIMTACC rgn:Glob, height 500 to 500 mb run at 0Z 2008-09-04 thru 2008-
- FIM rgn:Glob, height 500 to 500 mb run at 0Z 2008-09-04 thru 2008-09-15
- GFS rgn:Glob, height 500 to 500 mb run at 0Z 2008-09-04 thru 2008-09-15



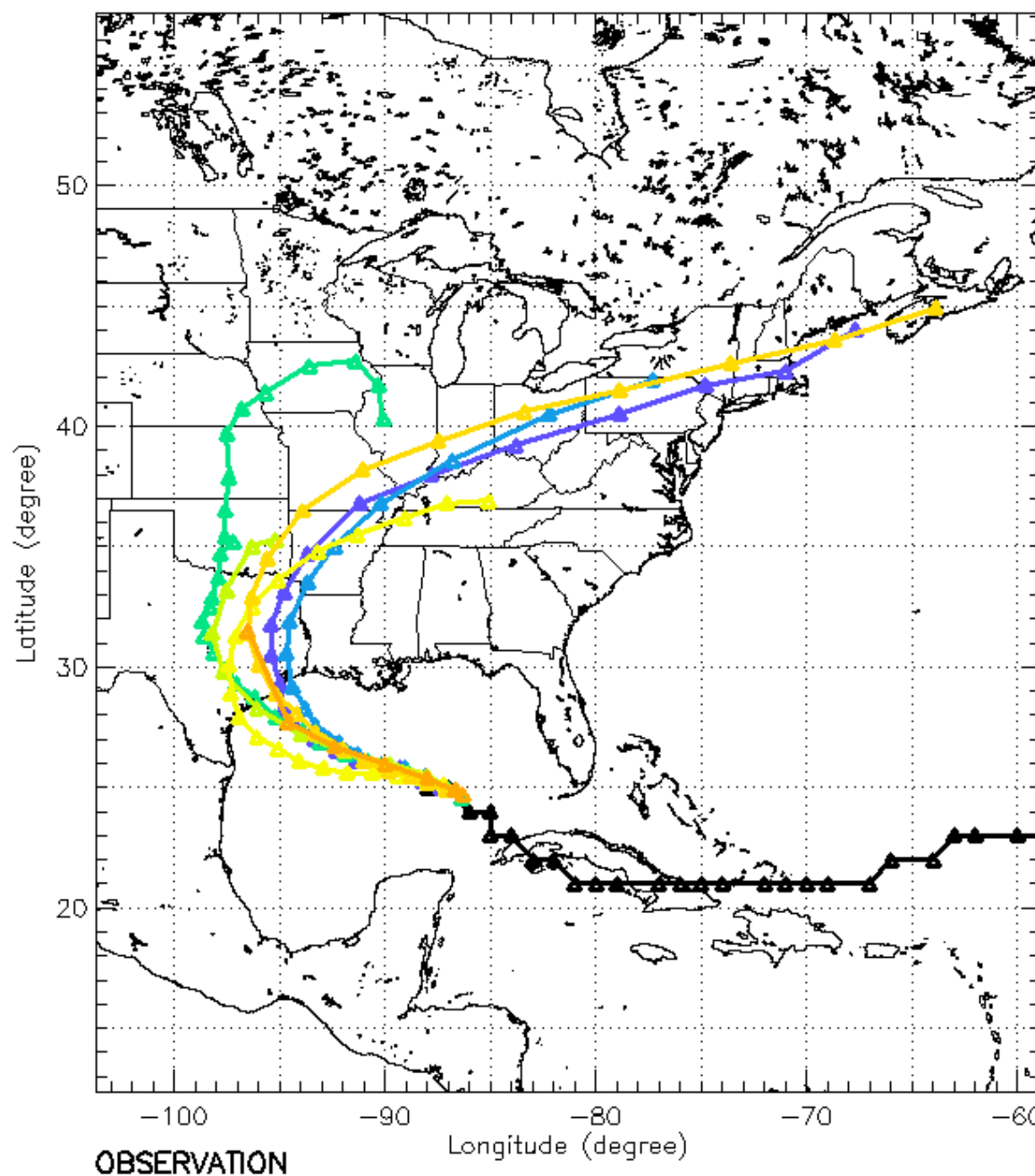
- FIMTACC rgn:Glob, height 500 to 500 mb run at 12Z 2008-09-06 thru 2008-09-1
- FIM rgn:Glob, height 500 to 500 mb run at 12Z 2008-09-06 thru 2008-09-1
- GFS rgn:Glob, height 500 to 500 mb run at 12Z 2008-09-06 thru 2008-09-1



Mass Conservation and Positive Definiteness

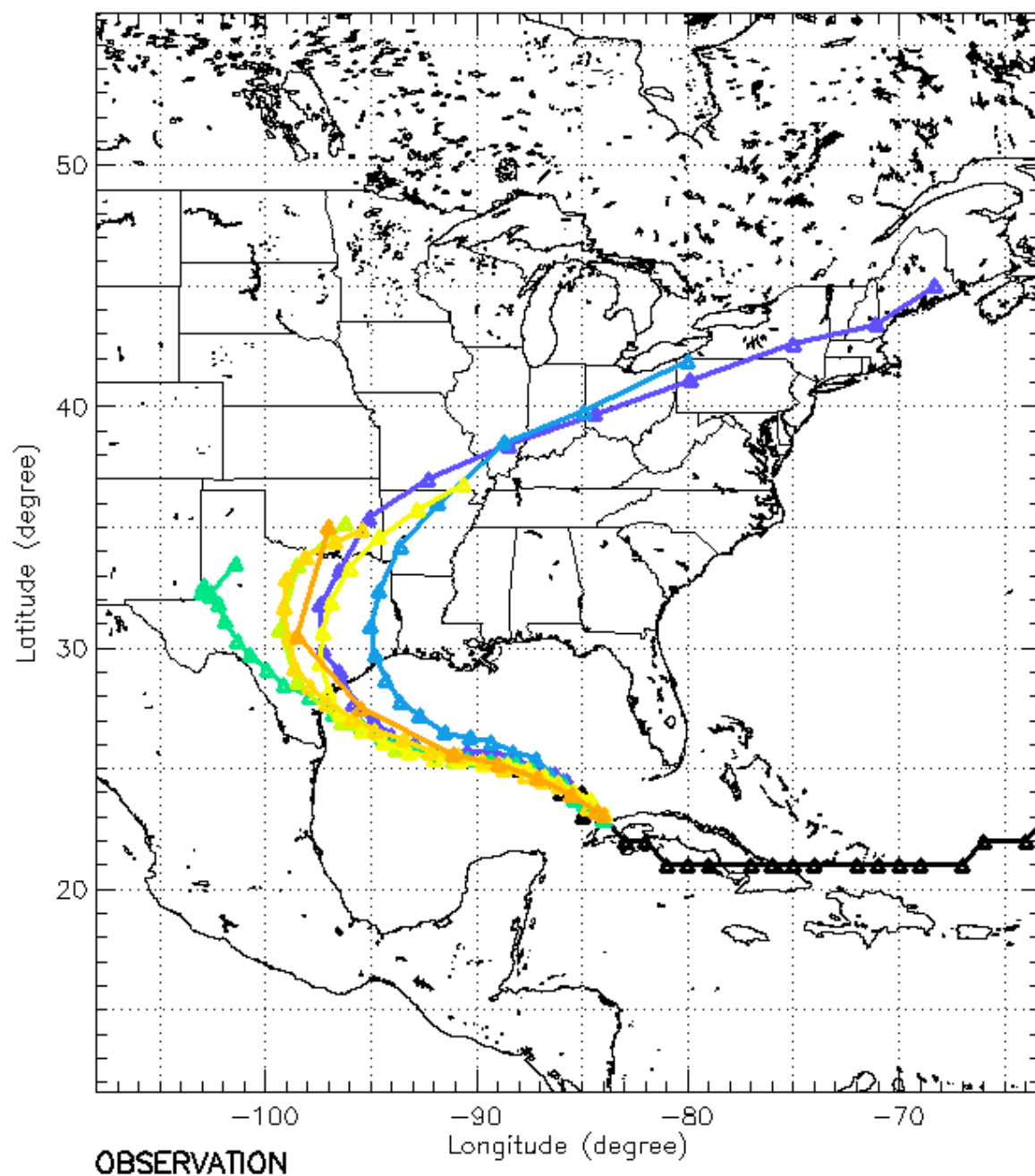
Integrated mass	= 5.022915528916858E+018 at time step=	1
Integrated mass	= 5.022915528916743E+018 at time step=	60
Integrated mass	= 5.022915528916771E+018 at time step=	120
Integrated mass	= 5.022915528916695E+018 at time step=	180
Integrated mass	= 5.022915528917074E+018 at time step=	240
Integrated mass	= 5.022915528917066E+018 at time step=	300
Integrated mass	= 5.022915528916768E+018 at time step=	360
Integrated mass	= 5.022915528916948E+018 at time step=	420
Integrated mass	= 5.022915528916820E+018 at time step=	480
Integrated mass	= 5.022915528916910E+018 at time step=	540
Integrated mass	= 5.022915528916967E+018 at time step=	600
Integrated mass	= 5.022915528916953E+018 at time step=	660
Integrated mass	= 5.022915528916784E+018 at time step=	720
Integrated mass	= 5.022915528916850E+018 at time step=	780
Integrated mass	= 5.022915528916886E+018 at time step=	840
Integrated mass	= 5.022915528916961E+018 at time step=	900
Integrated mass	= 5.022915528916819E+018 at time step=	960
Integrated mass	= 5.022915528916939E+018 at time step=	1020
Integrated mass	= 5.022915528916824E+018 at time step=	1080
Integrated mass	= 5.022915528916941E+018 at time step=	1140
Integrated mass	= 5.022915528916814E+018 at time step=	1200

HURRICANE IKE TRACK 2008 09 11 0000 UTC



Ike
Model tracks
- init 00z 11 Sep

HURRICANE IKE TRACK 2008 09 10 0000 UTC



Ike
Model tracks
- init 00z 10 Sep

- OFCL_091000
- GFDL_091000
- HWRF_091000
- AVNL_091000
- AVNO_091000
- FIM9_091000
- FIM8_091000

Development of NIM on Z-coord. (NIM: non-hydrostatic Icosahedral Model)

Preliminary Results

Compressible 2D Boussinesq eqs cast in flux form on Z-coord:

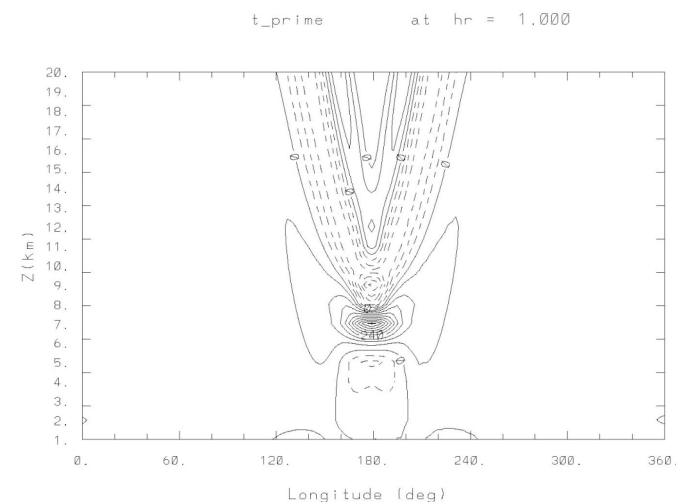
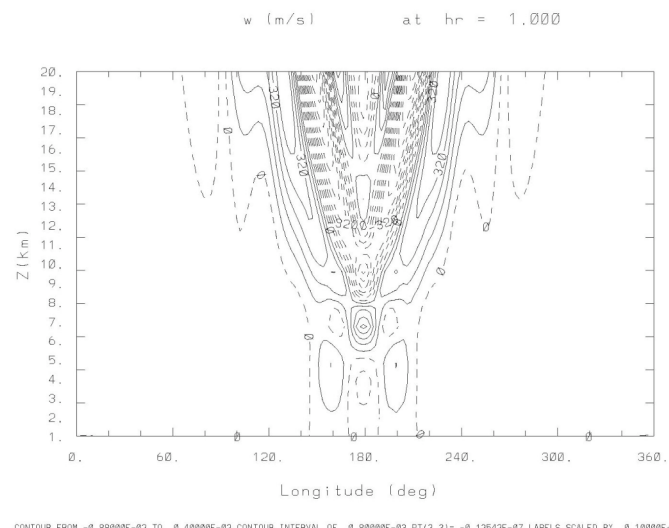
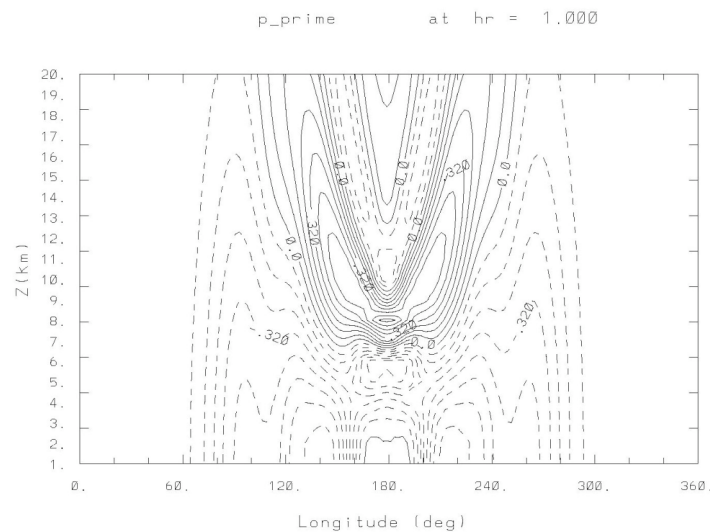
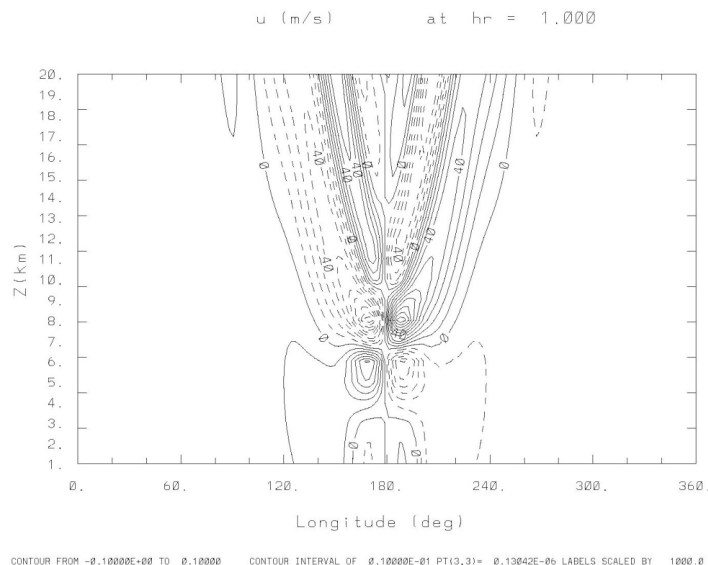
(A *simple* system which permits both gravity and acoustic waves)

$$\left\{ \begin{array}{l} \frac{\partial U}{\partial t} + \frac{\partial(Uu)}{\partial x} + \frac{\partial(Wu)}{\partial z} + \frac{\partial p'}{\partial x} = 0 \\ \frac{\partial W}{\partial t} + \frac{\partial(Uw)}{\partial x} + \frac{\partial(Ww)}{\partial z} + \left(\frac{\partial p'}{\partial z} \right) g \frac{\Theta'}{\bar{\Theta}(z)} = 0 \\ \frac{\partial \Theta'}{\partial t} + \frac{\partial(U\theta')}{\partial x} + \frac{\partial(W\theta')}{\partial z} + \frac{N^2}{g} W \bar{\theta}(z) = \frac{\Theta}{C_p} \frac{\dot{H}}{T} \\ \frac{\partial P'}{\partial t} + \frac{\partial(Up')}{\partial x} + \frac{\partial(Wp')}{\partial z} + \gamma P \left(\frac{\partial u}{\partial x} + \left(\frac{\partial w}{\partial z} \right) \right) = 0 \end{array} \right.$$

$$(U, W, \Theta, P) = (\rho u, \rho w, \rho \theta, \rho p), \quad \theta(x, z, t) = \bar{\theta}(z) + \theta'(x, z, t)$$

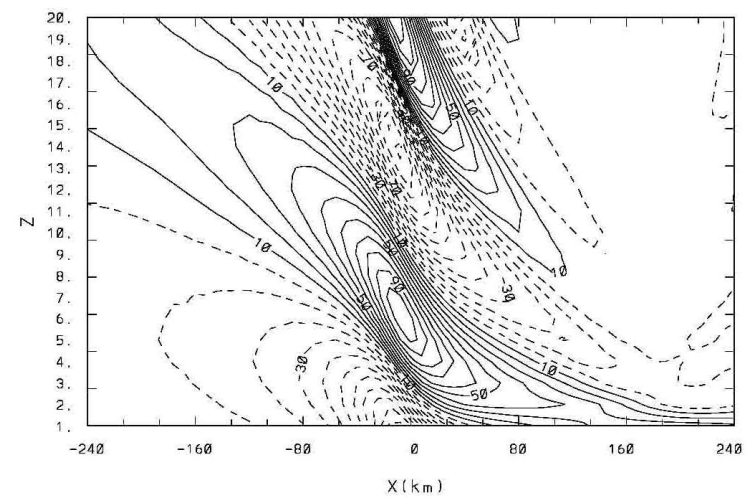
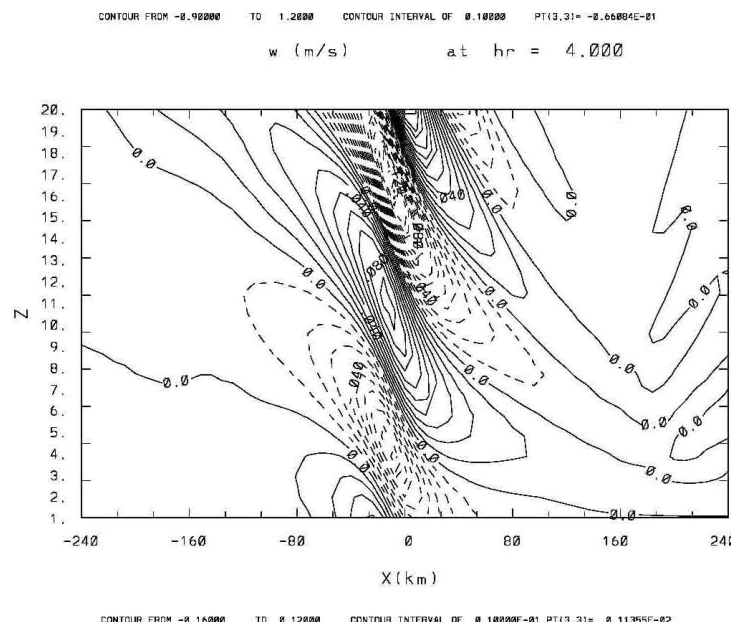
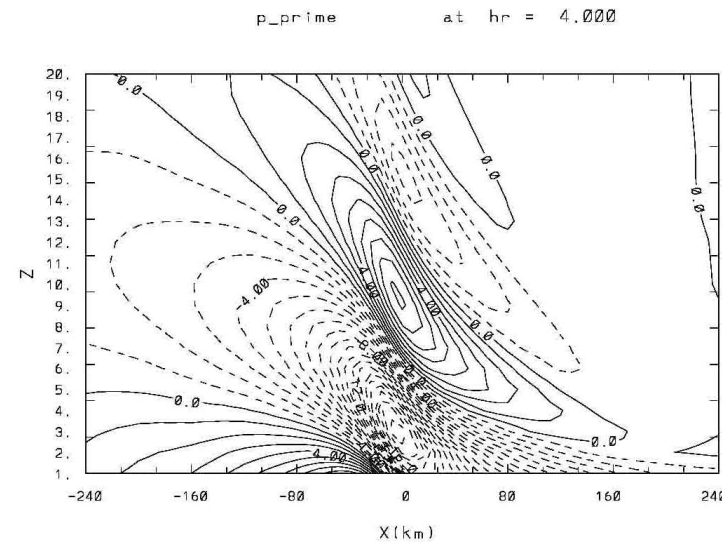
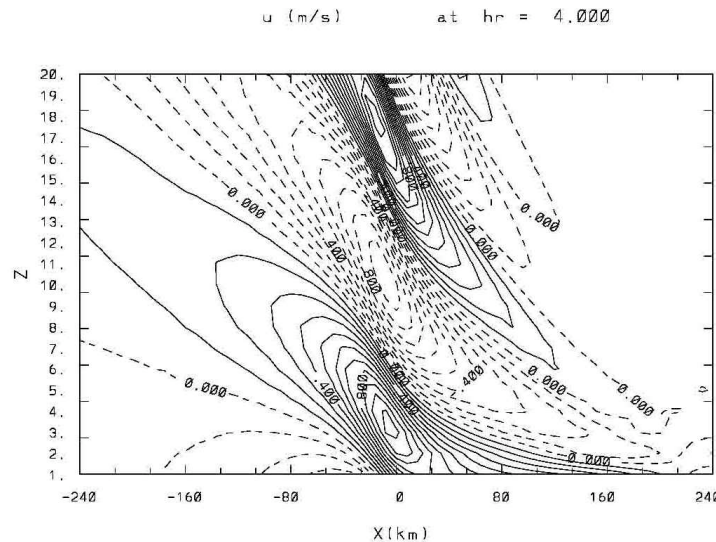
$$p(x, z, t) = \bar{p}(z) + p'(x, z, t); \quad \rho(x, z, t) = \bar{\rho}(z) + \rho'(x, z, t)$$

Heating excited vertical fast waves (explicit treatment)



dx=dz=1-km, dt=1sec, I.C: state of rest.

Numerical experiment on Mountain waves



$\text{dx}=8\text{km}$, $\text{dz}=1\text{-km}$, $\text{dt}=1\text{sec}$, $\text{U}=20\text{m/s}$, $Z_s=100\text{m}$, $L=30\text{km}$

Issues related to Icosahedral-Hexagonal grids

- Icos-grid noises (grid imprinting):
 1. *grid optimization algorithms available to reduce grid noises,*
 2. *numerical accuracy dependent,*
 3. *relatively small compared to other geodesic grids.*
- Conservation .vs. Accuracy
 1. *Mass conservation.*
 2. *Typically, the 2nd-order numerical accuracy.*
The 3rd-order scheme is desirable.
- Grid staggering issues :
A-grid with derivatives estimated using Vandermonde stencil points including center points (linear analysis?), C-grid ?
- Grid nesting issues:
Nesting ? Stretching grid ?